Inorganic Chemistry

Article

pubs.acs.org/IC

Thallium Mercury Chalcobromides, $TlHg_6Q_4Br_5$ (Q = S, Se)

Arief C. Wibowo,[†] Christos D. Malliakas,[†,‡] Duck Young Chung,[†] Jino Im,[§] Arthur J. Freeman,[§] and Mercouri G. Kanatzidis*[,†,‡]

[†]Materials Science Division, Argonne National Laboratory, Argonne, Illinois 60439, United States

[‡]Department of Chemistry and [§]Department of Physics and Astronomy, Northwestern University, Evanston, Illinois 60208, United States

Supporting Information

ABSTRACT: The new compounds $TlHg_6Q_4Br_5$ (Q = S, Se) are reported along with their syntheses, crystal structures, and thermal and optical properties, as well as electronic band structure calculations. Both compounds crystallize in the tetragonal $I4/m$ space group with a = 14.145(1) Å, c = 8.803(1) Å, and d_{calc} = 7.299 g/cm^3 for $TlHg_6S_4Br_5$ (compound **1**) and a = 14.518(2) Å, c = 8.782(1) Å, and d_{calc} = 7.619 g/cm^3 for $TlHg_6Se_4Br_5$ (compound **2**). They consist of cuboid $Hg_{12}Q_8$ building units interconnected by trigonal pyramids of $BrHg_3$, forming a three-dimensional structure. The interstitial spaces are filled with thallium and bromide ions. Compounds **1** and **2** melt incongruently and show band gaps of 3.03 and 2.80 eV, respectively, which agree well with the calculated ones. First-principles electronic structure calculations at the density functional theory level reveal that both compounds have indirect band gaps, but there also exist direct transitions at energies similar to the indirect gaps.

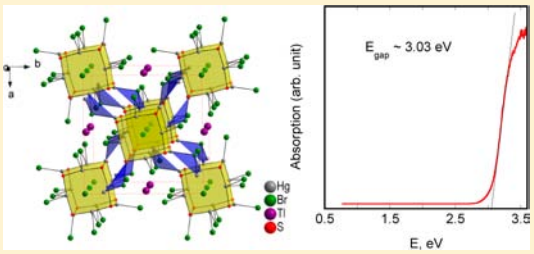

INTRODUCTION

Chalcohalide compounds are hybrids of a chalcogenide and a halide, with energy band gaps generally between those of the respective chalcogenide and halide.[1] Earlier we have proposed that chalcohalide may possess attractive physical properties, e.g., X-ray and γ-ray detection.[1j,m,2] The chalcohalide class of compounds has already demonstrated strong optical nonlinearity,[3] ferroelectricity,[4] phase transitions,[5] and upconversion luminescence.[6] We are interested in exploring highly dense, heavy-element containing chalcohalides, such as mercury and thallium, as part of a search for candidates for room temperature X-ray and γ-ray semiconductor detectors. Generally, the density and energy band gap of potential candidate materials for such purpose should be over 5 g/cm^3 and 1.6 eV, respectively, and preferably crystallizing in a three-dimensional compact structure in a high symmetry. The work reported here was motivated by the desire to identify new materials with prerequisites for hard radiation detectors, as mentioned above.

Mercury(II) adopts a closed shell electronic configuration and has a large ionic radius with flexible coordination environments, giving rise to diverse molecular architectures.[7] Thallium(I), with its $6s^2$ electronic configuration, often resembles the chemistry of alkali metal ions; hence, it is called the pseudoalkali metal.[8] Its so-called inert $6s^2$ electron pair can lead to a distorted local structure,[8,9] and its high atomic number can give high-density compounds.[1d,j,k,10] Therefore, semiconducting compounds that contain mercury and thallium are of interest as potential materials for X-ray and γ-ray semiconductor detectors. Recent reports on quaternary mercury-based chalcohalides include $[Hg_3Te_2][UCl_6]$,[11] $[Hg_3Q_2][MX_6]$ (Q = S, Se; M = Zr, Hf; X = Cl, Br),[7c] Hg_3AsQ_4X (Q = S, Se; X = Cl, Br, I),[7b] $Hg_3ZnS_2Cl_4$,[12] $[Hg_8As_4][Bi_3Cl_{13}]$,[13] $(Hg_2Cd_2S_2Br)Br$,[14] $Hg_7InS_6Cl_5$,[15] $Hg_2PbS_2I_2$,[16] and $Hg_3Q_2Bi_2Cl_8$ (Q = S, Se, Te).[7a] Herein, we report new thallium−mercury-based chalcohalides, $TlHg_6S_4Br_5$ (**1**) and $TlHg_6Se_4Br_5$ (**2**), with wide band gaps and high mass density. We describe their syntheses, structural characterization, and thermal and optical properties, as well as electronic structure, to evaluate their potentials to grow as large single crystals for room temperature X-ray and γ-ray semiconductor detector based on the criteria above.

EXPERIMENTAL SECTION

Chemicals in this work were used without further purification: $HgBr_2$ (99.998% metal basis, Sigma-Aldrich), TlBr (99.999% metal basis, Strem Chemicals, Inc.), elemental Hg (99.999%, electronic grade, Sigma-Aldrich), sulfur chunks (99.999%, Spectrum Chemical Mfg. Corp.), and selenium shots (99.999%, Plasmaterials). All manipulations were done inside a nitrogen-filled glovebox.

Synthesis of HgQ (Q = S, Se). HgS, a total of 10 g, was prepared as a stoichiometric mixture of mercury metal and sulfur powder. Liquid mercury was added by pipetting a stoichiometric amount into a fused silica tube and then sulfur was loaded. The tube was flame-sealed under a dynamic vacuum of ~10^{-4} mbar and then put into a programmable furnace. The mixture was heated to 400 °C over 12 h and held isothermally for 1 d, followed by cooling slowly to 50 °C over 6 h. The obtained dark red ingot was ground to powder before use. The product's purity was confirmed using powder X-ray diffraction (PXRD). A similar preparation procedure was adopted for HgSe,

Received: June 4, 2013
Published: October 9, 2013

Table 1. Crystal Data and Structure Refinement details for 1 and 2 at 293(2) K

	1	2
empirical formula	$TlHg_6S_4Br_5$	$TlHg_6Se_4Br_5$
formula weight	1935.70	2123.30
wavelength (Å)	0.71073 Å	
crystal system	tetragonal	
space group	$I4/m$	
unit cell dimensions	a = 14.145(1) Å, c = 8.803(1) Å	a = 14.518(2) Å, c = 8.782(1) Å
volume (Å^3)	1761.5(5)	1851.0(5)
Z	4	4
density (calcd) (g/cm^3)	7.299	7.619
abs coeff (mm^{-1})	72.99	76.87
F(000)	3200	3488
crystal size (mm^3)	0.05 × 0.03 × 0.02l	0.03 × 0.02 × 0.02
index ranges	$-16 \le h \le 16$, $-16 \le k \le 16$, $-9 \le l \le 9$	$-17 \le h \le 17$, $-17 \le k \le 17$, $-9 \le l \le 10$
reflections collected	5452	5742
independent reflections	802 (R_{int} = 0.1225)	875 (R_{int} = 0.1702)
completeness to θ = 24.97°	97.0%	99.7%
refinement method	full-matrix least-squares on F^2	
data/restraints/parameters	802/0/43	875/0/43
GOF	1.179	1.284
final R indices [$I > 2\sigma(I)$]	R_{obs} = 0.0439, wR_{obs} = 0.1045	R_{obs} = 0.0505, wR_{obs} = 0.1191
R indices (all data)[a]	R_{all} = 0.0653, wR_{all} = 0.1481	R_{all} = 0.0772, wR_{all} = 0.1650
largest diff. peak and hole (eÅ^{-3})	2.452 and −2.487	2.214 and −2.902

[a] $R = \sum||F_o| - |F_c||/\sum|F_o|$. $wR_2 = \{\sum[w(F_o^2 - F_c^2)]/\sum[w(F_o^2)]\}^{1/2}$.

which was heated to 550 °C over 16 h, held isothermally for 1 d, and then cooled slowly to 50 °C over 6 h. ***Caution!*** *Handling of mercury should be carried out in a fume hood or a glovebox. Heating the mixture of mercury and sulfur/selenium should be done slowly to ensure that the liquid mercury reacts with sulfur or selenium without evaporating.*

Synthesis of $TlHg_6S_4Br_5$ (1) and $TlHg_6Se_4Br_5$ (2). A ground mixture of HgQ (Q = S, Se) (4 mmol), $HgBr_2$ (2 mmol), and TlBr (1 mmol) totaling 0.5 g was loaded into a fused silica tube. The tube was flame-sealed under vacuum (~10^{-4} mbar) and was heated in a furnace to 200 °C over 6 h and held isothermally for 12 h for **1** or 48 h for **2**, followed by a shutdown of the furnace. Quantitative yields of polycrystalline powders of **1** (white with slight yellow tint) and **2** (pale yellow) were obtained.

To obtain a suitable size of high-quality single crystals for X-ray structural characterization, a separate synthetic reaction with a 1:1 mixture of HgQ and TlBr was carried out as follows. A thoroughly mixed powder of HgQ and TlBr at a 1:1 ratio totaling 0.5 g was sealed in a fused silica tube under vacuum, heated to 450 °C over 6 h and held isothermally for 6 h, and then heating to 750 °C for 6 h and held isothermally for 12 h. The tube was then cooled down slowly to 200 °C over 36 h and finally to room temperature within 1 h. The well-formed crystals of the quaternary compounds were produced approximately at 40% yield based on HgQ. A quantitative analysis of the crystals obtained was performed by scanning electron microscope-energy dispersive spectrometry (SEM-EDS).

Single-Crystal X-ray Diffraction. Single crystal XRD data were collected at 293 K on a STOE 2T image plate diffractometer with Mo Kα radiation (λ = 0.710 73 Å). An analytical absorption correction was applied to the data using the program X-Red on an optimized shape obtained with the aid of X-Shape software. The structures were solved by direct methods and refined with the SHELXTL software package. The displacement parameters were anisotropically refined for all atomic positions. Data were collected on several single crystals, to check for consistency in the lattice parameters. The complete data collection parameters and details of the structure solution and refinement for the compounds are given in Table 1. The fractional coordinates, the displacement parameters (U_{eq}), and occupancies of all atoms with estimated standard deviations are given in Tables 2 and S1 (Supporting Information). The selected bond lengths and angles are given in Table 3 for **1** and **2**.

Table 2. Atomic Coordinates (×10^4) and Equivalent Isotropic Displacement Parameters (Å^2 × 10^3) at 293(2) K with Estimated Standard Deviations in Parentheses

label	x	y	z	occupancy	U_{eq}[a]
		(a) $TlHg_6S_4Br_5$			
Tl	0	$^1/_2$	$^1/_4$	1	54(1)
Hg(1)	0.1768(1)	0.0378(1)	0.2639(2)	1	38(1)
Hg(2)	0.1428(2)	0.2302(2)	0	1	43(1)
S	0.1302(4)	0.2006(4)	0.2689(8)	1	27(2)
Br(1)	0	0	$^1/_2$	1	32(2)
Br(2)	0	0	0	1	34(2)
Br(3)	0.1724(2)	0.4293(2)	0	1	29(1)
Br(4)	0.3153(2)	0.0711(2)	0	1	33(1)
		(b) $TlHg_6Se_4Br_5$			
Tl	0	$^1/_2$	$^1/_4$	1	52(1)
Hg(1)	0.1769(1)	0.0395(1)	0.2640(2)	1	43(1)
Hg(2)	0.1380(2)	0.2383(2)	0	1	45(1)
Se	0.1309(2)	0.2048(2)	0.2800(3)	1	20(1)
Br(1)	0	0	$^1/_2$	1	25(2)
Br(2)	0	0	0	1	35(2)
Br(3)	0.1682(2)	0.4314(2)	0	1	25(1)
Br(4)	0.3145(2)	0.0692(3)	0	1	28(1)

[a] U_{eq} is defined as one-third of the trace of the orthogonalized U_{ij} tensor.

Powder X-ray Diffraction. PXRD patterns on the ground powder of the obtained products were collected using a PanAlytical X'Pert Pro powder diffractometer (Cu Kα radiation, λ = 1.5418 Å) over the 2θ range of 10°−70°, with a step size of 0.02° and a scan speed of 0.25°/min.

UV−Visible Spectroscopy. Optical diffuse-reflectance spectra were obtained at room temperature using a Shimadzu UV-3600 spectrophotometer operating in the 200−2500 nm region. The instrument is equipped with an integrating sphere and controlled by a personal computer. $BaSO_4$ was used as a 100% reflectance standard. The finely ground powder sample was spread on a compacted surface

dx.doi.org/10.1021/ic4014174 | Inorg. Chem. 2013, 52, 11875−11880

Table 3. Representative Bond Lengths (Å) and Bond Angles (deg)[a]

	$TlHg_6S_4Br_5$	$TlHg_6Se_4Br_5$
Bond Lengths		
Hg(1)−Q	2.395(5)	2.495(3)
Hg(1)−Q	2.401(5)	2.510(3)
Hg(1)−Br(3)	3.015(3)	3.088(3)
Hg(1)−Br(4)	3.075(3)	3.091(3)
Hg(2)-Q	2.410(7)	2.509(3)
Hg(2)-Q	2.410(7)	2.509(3)
Hg(2)−Br(3)	2.848(4)	2.837(4)
Q−Hg(1)	2.401(5)	2.511(3)
Br(3)−Hg(1)	3.015(3)	3.088(3)
Br(3)−Hg(1)	3.015(3)	3.088(3)
Br(4)−Hg(1)	3.075(3)	3.091(3)
Bond Angles		
Q−Hg(1)−Q	171.8(2)	171.0(1)
Q−Hg(1)−Br(3)	91.9(2)	91.4(1)
Q−Hg(1)−Br(3)	92.3(2)	88.9(1)
Q−Hg(1)−Br(4)	92.4(2)	94.6(1)
Q−-Hg(1)−Br(4)	94.4(2)	94.3(1)
Br(3)−Hg(1)−Br(4)	92.66(7)	90.77(8)
Q−Hg(2)−Q	158.2(3)	157.1(1)
Q−Hg(2)−Br(3)	100.5(1)	101.42(7)
Q−Hg(2)−Br(3)	100.5(1)	101.42(7)
Hg(1)−Q−Hg(1)	97.9(2)	96.9(1)
Hg(1)−Q−Hg(2)	97.4(2)	96.1(1)
Hg(1)−Q−Hg(2)	94.6(2)	91.0(1)
Hg(2)−Br(3)−Hg(1)	104.86(9)	104.3(1)
Hg(2)−Br(3)−Hg(1)	104.86(9)	104.3(1)
Hg(1)−Br(3)−Hg(1)	87.17(9)	84.3(1)
Hg(1)−Br(4)−Hg(1)	98.1(1)	97.2(1)

[a]Symmetry transformations used to generate equivalent atoms: (1) $y, -x, z$; (2) $-x + {}^1/_2, -y + {}^1/_2, -z + {}^1/_2$; (3) $x, y, -z$; (4) $-y, x, z$; (5) $-x + {}^1/_2, -y + {}^1/_2, z - {}^1/_2$.

of the standard material preloaded into a sample holder. The reflectance versus wavelength data generated were used to estimate the band gap of the material by converting reflectance to absorption data according to Kubelka−Munk equation: $\alpha/S = (1 - R)^2/(2R)$, where R is the reflectance and α and S are the absorption and scattering coefficients, respectively.[17]

Differential Thermal Analysis (DTA). Thermal behavior of the compounds was analyzed on a Shimadzu DTA-50. A sample (~30 mg) of ground powder was sealed in a silica ampule under vacuum. A silica ampule of equal mass filled with Al_2O_3 was sealed and placed on the reference side of the detector. The sample was heated to 430 or 500 °C at 5 °C/min, and after 10 min it was cooled at a rate of −5 °C/min to 50 °C. One or two cycles of heating and cooling were applied to the sample. The residues from the DTA experiments were examined by PXRD.

Band Structure Calculations. To investigate the electronic structures of both compounds, first-principles calculations were performed within the density functional theory (DFT) formalism using the projector augmented wave (PAW) method[18] implemented in the Vienna Ab-initio Simulation Package (VASP) code.[19] The cutoff energy of the planewave basis was set to 350 eV, and 5 × 5 × 5 regular k-point meshes were used for the Brillouin zone sampling. In order to evaluate the band gap accurately, we employed the hybrid functional within the Heyd−Scuseria−Ernzerhof (HSE) approach,[20] which leads to a good agreement with experimentally measured band gaps.[21]

RESULTS AND DISCUSSION

Synthesis. Air stable, isotypic compounds of the formula $TlHg_6Q_4Br_5$ (Q = S, Se) were first identified by the reactions of mercury chalcogenides with thallium bromide in a closed silica ampule under a temperature of 750 °C. After discovery of these new compounds, we attempted to optimize the synthetic conditions to obtain quantitative yields using a stoichiometric mixture of HgQ (Q = S, Se), $HgBr_2$, and TlBr. The experiments involved two types of heat treatments such as (a) melting and slow cooling and (b) melting and quenching in ice water. None of these synthetic attempts were successful in giving a single phase product of either compound. Instead, the ternary $Hg_3S_2Br_2$ or $Hg_3Se_2Br_2$ phases were always present as minor products in addition to small amounts of Tl_2S or HgSe.

A quantitative yield of both compounds was finally obtained by solid-state diffusion of each stoichiometric mixture at 200 °C. The PXRD patterns of the products obtained are shown in Figure 1 for **1** and **2**, showing pure phase of both compounds. The peak positions of these isostructural compounds are slightly shifted from one another, as expected.

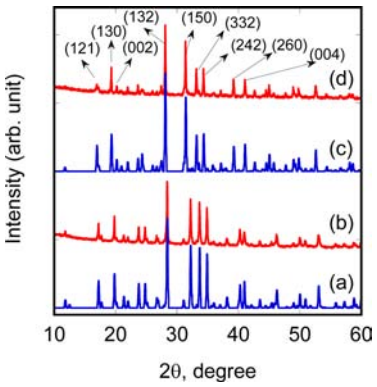

Figure 1. Powder X-ray diffraction patterns of (a) simulated and (b) observed pattern of **1** and (c) simulated and (d) observed pattern of **2** (Cu Kα radiation).

Attempts to synthesize the tellurium analogue using a stoichiometric reaction of HgTe, $HgBr_2$, and TlBr produced $Hg_3Te_2Br_2$, $HgTl_4Br_6$, and HgTe. Investigations aimed at synthesizing other quaternary chalcohalide analogues with different halides TlX (X = Cl, I) and different alkali bromides ABr (A = K, Rb, Cs) under similar conditions described above were also unsuccessful, yielding only the starting binaries and $Hg_3Q_2X_2$.

Structural Description. Both $TlHg_6Q_4Br_5$ (Q = S, Se) compounds are isostructural, consisting of $Hg_{12}Q_8$ cuboids interconnected in three dimensions by $BrHg_3$ trigonal pyramids; see Figure 2. Conceptually, the structure is derived from α-$Hg_3S_2Br_2$[7f,22] (Figure 2a) by incorporating 2 times the amount of atoms in the unit cell, hence $Hg_6Q_4Br_4$, while maintaining the cuboid units, $Hg_{12}Q_8$, as the main building unit. Tl and Br ions fill the remaining interstitial space to complete the observed quaternary structures, $TlHg_6Q_4Br_5$ (Q = S, Se). There are significant differences between α-$Hg_3S_2Br_2$ and $TlHg_6Q_4Br_5$ in terms of how the cuboid units are connected. The former cuboid units and their surroundings have $2/m$ symmetry (Figure 2a), whereas the latter have $4/m$ symmetry (Figure 2b). These cuboids are linked into a three-dimensional structure. There are three types of linkers in α-$Hg_3S_2Br_2$, which consist of $Br(3)Hg_3$ (orange color) and Br(4)Hg3 (turquoise color) trigonal pyramids and Br(5) atoms (Figure 2a). In $TlHg_6Q_4Br_5$, however, only one linker,

dx.doi.org/10.1021/ic4014174 | Inorg. Chem. 2013, 52, 11875−11880

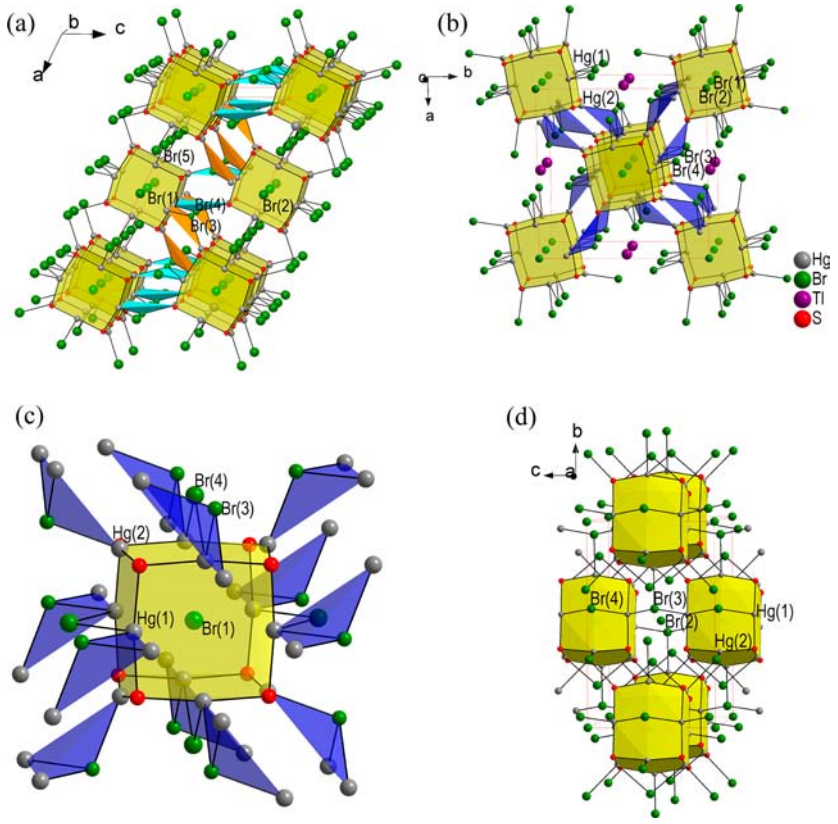

Figure 2. (a) A representative 3D structure of α-$Hg_3S_2Br_2$ showing 2/*m* symmetry.[22b] (b) A representative 3D structure of $TlHg_6S_4Br_5$ along the *c*-axis, showing 4/*m* symmetry. (c) A cuboid unit, $Hg_{12}S_8$, in $TlHg_6Q_4Br_5$ with its detailed environments, and (d) view along the *a*-axis, showing Br(2) located in between adjacent cuboid units similar to that in α-$Hg_3S_2Br_2$. Br(1) is located in the center of cuboid unit (not shown).

$Br(3)Hg_3$ (blue color in Figure 2b) trigonal pyramids, is observed.

The cuboid units $Hg_{12}Q_8$ (Q = S, Se) of $TlHg_6Q_4Br_5$ shown in Figure 2c are built from eight QHg_3 trigonal pyramids with S or Se atoms located in the cuboid corners, similar to the ones in α-$Hg_3S_2Br_2$. Each S/Se forms the trigonal pyramid with two Hg(1) and one Hg(2). S−Hg bond distances ranging from 2.395(5) to 2.410(7) Å and Se−Hg bond distances ranging from 2.495(3) to 2.511(3) Å are observed for **1** and **2**, respectively. In the same manner as the ones in α-$Hg_3S_2Br_2$, Br(1) atoms of $TlHg_6Q_4Br_5$ are located in the center of $Hg_{12}Q_8$ cuboids, and Br−Hg bond distances ranging from 2.837(4) to 3.091(3) Å and Br−Q bond distances ranging from 3.89(5) to 4.301(3) Å are observed in compounds **1** and **2**. In Figure 2d, Br(2) atoms are located in between adjacent cuboid units, similar to that of α-$Hg_3S_2Br_2$, with bond distances of 3.455(1) and 3.507(2) Å from neighboring Hg(1) atoms observed in **1** and **2**, respectively. The blue trigonal pyramids (Figure 2b,c), which connect the cuboid units in three dimensions, consist of Br(3) surrounded by two Hg(1) and one Hg(2) with bond distances ranging from 2.838(4) to 3.087(3) Å in both compounds. Br(4) atoms bridge two Hg(1) atoms within a cuboid unit with bond distance of 3.075(2) and 3.091(2) Å for **1** and **2**, respectively. The Tl atoms are eight-coordinated, with Br(3) and Br(4) atoms forming a slightly distorted cube with Tl−Br bond distances ranging from 3.432(2) to 3.617(3) Å in compounds **1** and **2** (Figure S1, Supporting Information).

Thermal Properties. The thermal behavior of **1** and **2** was investigated by two consecutive cycles of heating and cooling in DTA. Compound **1** exhibits a broad endothermic peak at ∼466 °C (melting point) on heating and exothermic peaks at ∼436 °C (crystallization point) on cooling (Figure S2a, Supporting Information). Similarly, compound **2** exhibits a broad endothermic peak at ∼495 °C (melting point) and exothermic peaks at ∼462 °C (crystallization point) (Figure S2b, Supporting Information). In two cycles of heating/cooling, there are slight shifts in melting point (for **1**) and crystallization point (for **2**). This behavior indicates that the compounds **1** and **2** are incongruent-melting, as often observed in other mercury chalcohalides.[7a,c,15] The incongruent-melting behavior of both compounds is further confirmed by PXRD patterns on the residues of DTA measurements (Figure S3 and S4 (Supporting Information) for **1** and **2**, respectively). In these PXRD patterns, we observed the decomposition products $Hg_3Q_2Br_2$, $HgTl_4Br_6$, and HgQ, as well as $TlHg_6Q_4Br_5$ (Q = S, Se), which may be attributed to eq 1:

$$4TlHg_6Q_4Br_5 \xrightarrow{\triangle} 7Hg_3Q_2Br_2 + Tl_4HgBr_6 + 2HgQ \quad (Q = S, Se) \qquad (1)$$

In addition, there are minute endothermic and exothermic peaks that appeared and/or disappeared during two cycles of heating and cooling in compound **2** (Figure S4, Supporting Information, labeled by arrows for clarity) that cannot be attributed to the starting reagents nor be identified from the PXRD pattern of the pristine compound, as indicated in Figure 2. There may be a possibility that this compound decomposes before melting, which may correlate with the observed decomposed products, eq 1 above, of the DTA residue. We attempted to clarify these minute peaks by heating the sample

dx.doi.org/10.1021/ic4014174 | *Inorg. Chem.* 2013, 52, 11875−11880

to 430 °C and then cooling down to room temperature followed by PXRD examination. Although the sample turns dark after such heating, the PXRD pattern still shows pure $TlHg_6Se_4Br_5$. Further investigation on this matter is underway in order to optimize the conditions for a large-scale synthesis and high-quality crystal growth required for a feasibility test for hard radiation detectors.

Optical Properties. Diffuse reflectance UV−vis/near-IR (NIR) spectra collected for both **1** and **2** at room temperature show well-defined, sharp absorption edges. The band gap of **1** is ∼3.03 eV (Figure 3a), in accordance with the color (white with

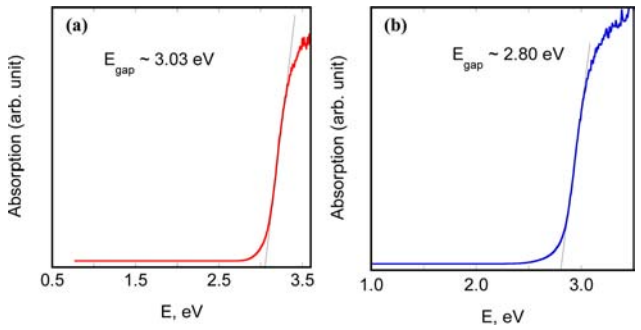

Figure 3. Optical absorption spectra of (a) **1** and (b) **2**, measured at room temperature.

slight yellow tint) of the plate crystals obtained. The spectrum of compound **2** (Figure 3b) shows a band gap of 2.80 eV, as expected from the yellow-colored plate crystals obtained. The sharp characters of the absorption edges are suggestive of direct transitions, supported by the electronic band structure calculations below.

Band Structure. To understand the nature of the band gap of compounds **1** and **2**, we performed first-principles electronic structure calculations using the HSE functional. As shown in Figure 4a,b, the band structures of both compounds are similar to each other. In both compounds, the band gaps are predicted to be indirect; the conduction band minima (CBM) of both compounds are located at the Γ points of the Brillouin zone, while the valence band maxima (VBM) occur at the X points. However, the direct transitions between the valence band and the conduction band at Γ show band gaps (3.08 eV for **1** and 2.89 eV for **2**) that are very close in energy to the calculated indirect band gaps (3.00 eV for **1** and 2.74 eV for **2**). This result implies that the sign of the indirect band gap is hidden by the direct transition, which has much higher amplitude than that of indirect transition in an optical spectrum measurement, and thus, it can explain the sharp absorption edges in Figure 3. The calculated direct band gaps agree well with the experimentally measured ones (3.03 eV for **1** and 2.80 eV for **2**).

From the projected density of states (PDOS) in Figure 5a,b, we find that VBM of both compounds mainly consist of Br p

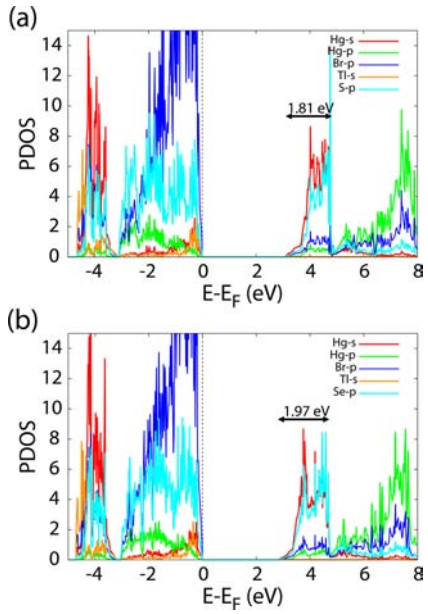

Figure 5. Calculated projected density of states (PDOS) of (a) **1** and (b) **2**. In all plots, the E_F is set to the energy of the valence band maximum. Red, green, blue, and orange curves correspond to Hg s, Hg p, Br p, and Tl s orbitals, respectively; S p and Se p orbitals are plotted by turquoise curves in parts a and b.

orbitals and S/Se p orbitals, while Hg s orbitals and S/Se p orbitals mostly contribute to CBM. Compared to the VBM, the CBM has s-orbital symmetry due to the strong contribution of the Hg s orbital, resulting in a more dispersive conduction band of both compounds, as shown in Figure 4a,b. In addition, the bandwidth of the conduction band located at $E-E_F$ = 3−5 eV increases from 1.81 eV in **1** to 1.97 eV in **2** due to the more extended character of the Se p orbital than the S p orbital (see Figure 5). This result can explain the band gap difference of

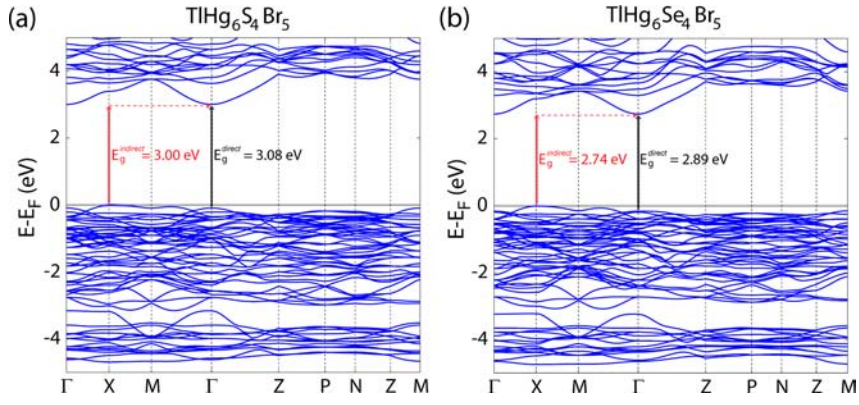

Figure 4. Calculated electronic band structures of (a) **1** and (b) **2**. In all plots, the E_F is set to the energy of the valence band maximum. Indirect gaps and direct gaps are denoted by red and black arrows, respectively.

dx.doi.org/10.1021/ic4014174 | Inorg. Chem. 2013, 52, 11875−11880

compounds **1** and **2** found in the optical measurements (Figure 3).

CONCLUSIONS

Two new quaternary mercury- and thallium-based chalcohalides with general formula $TlHg_6Q_4Br_5$ (Q = S, Se) were synthesized at low temperatures by solid-state diffusion. Both compounds exhibit important features, displaying three-dimensional structures with high symmetry (*I*4/*m* space group), high specific density (7.299 g/cm^3 for **1** and 7.619 g/cm^3 for **2**), high atomic numbers, and wide energy gaps of 3.03 and 2.80 eV for **1** and **2**, respectively, which meet the prerequisites for X-ray and γ-ray detection applications. First-principles electronic structure calculations reveal that both compounds have an indirect band, but with near-lying direct transitions, which are responsible for the sharp absorption edges observed in the optical spectrum. The calculated direct band gaps predict 3.08 eV for **1** and 2.89 eV for **2**, which agrees well with the experimental results. Growing large-size single crystals of these compounds using the Bridgman technique, which is challenging due to the incongruent melting nature of both compounds, is currently underway for further investigation in X-ray and γ-ray detection.

ASSOCIATED CONTENT

Supporting Information

Further details are given in Table S1 and Figures S1−S4, as noted in the text, and crystallographic data are given in CIF format. This material is available free of charge via the Internet at http://pubs.acs.org.

AUTHOR INFORMATION

Corresponding Author

*E-mail: m-kanatzidis@northwestern.edu.

Notes

The authors declare no competing financial interest.

ACKNOWLEDGMENTS

This work was supported by the Office of Nonproliferation and Verification Research and Development under National Nuclear Security Administration of the U.S. Department of Energy under Contract No. DE-AC02-06CH11357.

REFERENCES

(1) (a) Beck, J.; Dolg, M.; Schluter, S. *Angew. Chem., Int. Ed.* **2001**, *40*, 2287−2290. (b) Deiseroth, H.-J.; Kong, S.-T.; Eckert, H.; Vannahme, J.; Reiner, C.; Zaib, T.; Schlosser, M. *Angew. Chem., Int. Ed.* **2008**, *47*, 755−758. (c) Gunther, A.; Heise, M.; Wagner, F. R.; Ruck, M. *Angew. Chem., Int. Ed.* **2011**, *50*, 9987−9990. (d) Long, J. R.; Williamson, A. S.; Holm, R. H. *Angew. Chem., Int. Ed. Engl.* **1995**, *34*, 226−229. (e) Pfitzner, A.; Reiser, S.; Nilges, T. *Angew. Chem., Int. Ed.* **2000**, *39*, 4160−4162. (f) Gabriel, J.-C. P.; Boubekeur, K.; Uriel, S.; Batail, P. *Chem. Rev.* **2001**, *101*, 2037−2066. and references therein (g) Kabbour, H.; Cario, L. *Inorg. Chem.* **2006**, *45*, 2713−2717. (h) Sokolov, M. N.; Gushchin, A. L.; Abramov, P. A.; Virovets, A. V.; Peresypkina, E. V.; Fedin, V. P. *Inorg. Chem.* **2007**, *46*, 4677−4682. (i) Biswas, K.; Zhang, Q.; Chung, I.; Song, J.-H.; Androulakis, J.; Freeman, A. J.; Kanatzidis, M. G. *J. Am. Chem. Soc.* **2010**, *132*, 14760−14762. (j) Johnsen, S.; Liu, Z.; Peters, J. A.; Song, J.-H.; Nguyen, S.; Malliakas, C. D.; Jin, H.; Freeman, A. J.; Wessels, B. W.; Kanatzidis, M. G. *J. Am. Chem. Soc.* **2012**, *133*, 10030−10033. (k) Long, J. R.; McCarty, L. S.; Holm, R. H. *J. Am. Chem. Soc.* **1996**, *118*, 4603−4616. (l) Smith, M. D.; Miller, G. J. *J. Am. Chem. Soc.* **1996**, *118*, 12238−12239. (m) Malliakas, C. D.; Wibowo, A. C.; Liu, Z.; Peters, J. A.; Sebastian, M.; Jin, H.; Chung, D.-Y.; Freeman, A. J.; Wessels, B. W.; Kanatzidis, M. G. *Proc. SPIE* **2012**, *8507*, 14.

(2) Androulakis, J.; Peter, S. C.; Li, H.; Malliakas, C. D.; Peters, J. A.; Liu, Z.; Wessels, B. W.; Song, J.-H.; Jin, H.; Freeman, A. J.; Kanatzidis, M. G. *Adv. Mater.* **2011**, *23*, 4163−4167.

(3) (a) Cai, Y.; Wang, Y.; Li, Y.; Wang, X.; Xin, X.; Liu, C.; Zheng, H. *Inorg. Chem.* **2005**, *44*, 9128−9130. (b) Guo, S.-P.; Guo, G.-C.; Wang, M.-S.; Zou, J.-P.; Zeng, H.-Y.; Cai, L.-Z.; Huang, J.-S. *Chem. Commun.* **2009**, 4366−4368. (c) Zhang, Q.; Chung, I.; Jang, J. I.; Ketterson, J. B.; Kanatzidis, M. G. *J. Am. Chem. Soc.* **2009**, *131*, 9896−9897.

(4) (a) Itoh, K.; Matsunaga, H.; Nakamura, E. *J. Phys. Soc. Jpn.* **1976**, *41*, 1679. (b) Xu, Z. C.; Fong, C. Y.; Wooten, F.; Yeh, Y. *Ferroelectrics* **1984**, *56*, 187.

(5) (a) Nilges, T.; Osters, O.; Bawohl, M.; Bobet, J.-L.; Chevalier, B.; Decourt, R.; Weihrich, R. *Chem. Mater.* **2010**, *22*, 2946−2954. (b) Kong, S.-T.; Deiseroth, H.-J.; Reiner, C.; Gun, O.; Neumann, E.; Ritter, C.; Zahn, D. *Chem.—Eur. J.* **2010**, *16*, 2198−2206. (c) Gagor, A.; Pietraszko, A.; Kaynts, D. *J. Solid State Chem.* **2005**, *178*, 3366−3375.

(6) (a) Xu, Y.; Chen, D.; Zhang, Q.; Zeng, H.; Shen, C.; Adam, J.-l.; Zhang, X.; Chen, G. *J. Phys. Chem. C.* **2009**, *113*, 9911−9915. (b) Wang, W.; Zhang, Q.; Xu, Y.; Shen, C.; Chen, D.; Chen, G. *J. Am. Ceram. Soc.* **2010**, *93*, 2445−2447.

(7) (a) Wibowo, A. C.; Malliakas, C. D.; Chung, D.-Y.; Im, J.; Freeman, A. J.; Kanatzidis, M. G. *Inorg. Chem.* **2013**, *52*, 2973−2979. (b) Beck, J.; Hedderich, S.; Kollisch, K. *Inorg. Chem.* **2000**, *39*, 5847−5850. (c) Beck, J.; Hedderich, S. *J. Solid State Chem.* **2003**, *172*, 12−16. (d) Axtell, E. A., III; Park, Y.; Chondroudis, K.; Kanatzidis, M. G. *J. Am. Chem. Soc.* **1998**, *120*, 124. (e) Kanatzidis, M. G.; Park, Y. *Chem. Mater.* **1990**, *2*, 99. (f) Magarill, S. A.; Pervukhina, N. V.; Borisov, S. V.; Pal'chik, N. A. *Russ. Chem. Rev.* **2007**, *76*, 101. (g) Beck, J.; Keller, H.-L.; Rompel, M.; Wimbert, L.; Ewald, B. *Z. Anorg. Allg. Chem.* **2004**, *630*, 1031. (h) Liao, J.-H.; Marking, G. M.; Hsu, K. H.; Matsushita, Y.; Ewbank, M. D.; Borwick, R.; Cunningham, P.; Rosker, M. J.; Kanatzidis, M. G. *J. Am. Chem. Soc.* **2003**, *125*, 9484.

(8) Timofte, T.; Mudring, A.-V. *Z. Anorg. Allg. Chem.* **2009**, *635*, 840.

(9) (a) Mudring, A.-V. *Eur. J. Inorg. Chem.* **2007**, *2007*, 882. (b) McGuire, M. A.; Reynolds, T. K.; DiSalvo, F. J. *Chem. Mater.* **2005**, *17*, 2875. (c) Teske, C. L.; Bensch, W. *Z. Anorg. Allg. Chem.* **2001**, *627*, 385.

(10) (a) Johnsen, S.; Liu, Z.; Peters, J. A.; Song, J.-H.; Peter, S. C.; Malliakas, C. D.; Cho, N. K.; Jin, H.; Freeman, A. J.; Wessels, B. W.; Kanatzidis, M. G. *Chem. Mater.* **2011**, *23*, 3120. (b) Huan, G.; Greaney, M.; Tsai, P. P.; Greenblatt, M. *Inorg. Chem.* **1998**, *28*, 2448.

(11) Bugaris, D. E.; Ibers, J. A. *J. Solid State Chem.* **2008**, *181*, 3189−3193.

(12) Chen, W.-T.; Kuang, H.-M.; Chen, H.-L. *J. Solid State Chem.* **2010**, *183*, 2411−2415.

(13) Jiang, X.-M.; Zhang, M.-J.; Zeng, H.-Y.; Guo, G.-C.; Huang, J.-S. *J. Am. Chem. Soc.* **2011**, *133*, 3410−3418.

(14) Zou, J.-P.; Peng, Q.; Luo, S.-L.; Tang, X.-H.; Zhang, A.-Q.; Zeng, G.-S.; Guo, G.-C. *CrystEngComm* **2011**, *13*, 3862−3867.

(15) Liu, Y.; Wei, F.; Yeo, S. N.; Lee, F. M.; Kloc, C.; Yan, Q.; Hng, H. H.; Ma, J.; Zhang, Q. *Inorg. Chem.* **2012**, *51*, 4414−4416.

(16) Blachnik, R.; Buchmeier, W.; Dreisbach, H. A. *Acta Crystallogr. C* **1986**, *42*, 515.

(17) (a) Kortum, G.; Braun, W.; Herzog, G. *Angew. Chem.* **1963**, *75*, 653. (b) McCarthy, T. J.; Kanatzidis, M. G. *Chem. Mater.* **1993**, *5*, 1061−1063. Liao, J. H.; Kanatzidis, M. G. *Chem. Mater.* **1993**, *5*, 1561−1569.

(18) Blochl, P. E. *Phys. Rev. B.* **1994**, *50*, 17953.

(19) Kresse, G.; Furthmuller, J. *Phys. Rev. B.* **1996**, *54*, 11169.

(20) Heyd, J.; Scuseria, G. E.; Ernzerhof, M. *J. Chem. Phys.* **2003**, *118*, 8207.

(21) Heyd, J.; Scuseria, G. E. *J. Chem. Phys.* **2004**, *121*, 1187.

(22) (a) Minets, Y. V.; Voroshilov, Y. V.; Pan'ko, V. V. *J. Alloys Compd.* **2004**, *367*, 109−114. (b) Voroshilov, Y. V.; Khudolii, V. A.; Pan'ko, V. V.; Minets, Y. V. *Neorg. Mater.* **1996**, *32*, 1461.